

Use of XAS for the Elucidation of Metal Structure and Function: Applications to Nickel Biochemistry, Molecular Toxicology, and Carcinogenesis

Paul E. Carrington,¹ Faizah Al-Mjeni,¹ Maria A. Zoroddu,² Max Costa,³ and Michael J. Maroney¹

¹Department of Chemistry, University of Massachusetts, Amherst, Massachusetts, USA; ²Department of Chemistry, University of Sassari, Sassari, Italy; ³Department of Environmental Medicine and Kaplan Comprehensive Cancer Center, New York University School

Nickel has been shown to be an essential trace element involved in the metabolism of several species of bacteria, archaea, and plants. In these organisms, nickel is involved in enzymes that catalyze both non-redox (e.g., urease, glyoxalase I) and redox (e.g., hydrogenase, carbon monoxide dehydrogenase, superoxide dismutase) reactions, and proteins involved in the transport, storage, metallocenter assembly, and regulation of nickel concentration have evolved. Studies of structure/function relationships in nickel biochemistry reveal that cysteine ligands are used to stabilize the Ni(III/II) redox couple. Certain nickel compounds have also been shown to be potent human carcinogens. A likely target for carcinogenic nickel is nuclear histone proteins. Here we present X-ray absorption spectroscopic studies of a model Ni peptide designed to help characterize the structure of the nickel complexes formed with histones and place them in the context of nickel structure/function relationships, to gain insights into the molecular mechanism of nickel carcinogenesis. **Key words:** carcinogenesis, enzyme, histone, nickel, nucleosome, protein, XAS. *Environ Health Perspect* 110(suppl 5):705–708 (2002).

<http://ehpnet1.niehs.nih.gov/docs/2002/suppl-5/705-708carrington/abstract.html>

Nickel is an essential metal for many archaea, bacteria, and plants (1), and may yet be found to play a role in the metabolism of higher organisms. Most bacteria and archaea that can live under anaerobic conditions (including beneficial bacteria in the human gut) produce several enzymes that require Ni. Yet, under some circumstances, Ni is a potent human carcinogen (2,3). As potential specific molecular targets for carcinogenic Ni are identified, it becomes possible to examine the structure of these Ni sites for clues to how they give rise to cancer. X-ray absorption spectroscopy (XAS) is one technique that provides detailed structural information regarding biological Ni sites. Analysis of Ni K-edge X-ray absorption near-edge structure (XANES) produces information regarding the coordination number and geometry of a Ni site (4). Comparison of shifts in Ni K-edge energies may reveal redox-active Ni sites. The analysis of extended X-ray absorption fine structure (EXAFS) provides information regarding the types of ligands bound to Ni and metric details for the Ni site (5,6). The main goal of this research is to provide structural information regarding biological Ni sites that are potentially involved in carcinogenesis, and to elucidate the likely properties that give rise to carcinogenesis by comparing these structures with those of Ni-containing biological molecules with known functions.

Structure/Function Relationships in Nickel Metallobiochemistry

A variety of Ni-binding proteins and Ni-dependent enzymes have been structurally characterized (Figure 1). As with most

transition metals, the uptake, transport, storage, intracellular concentration, and biosynthesis of Ni metalloenzymes are tightly regulated by proteins that specifically bind Ni(II). These proteins include examples of Ni-specific permeases (e.g., NixA, HoxN, NikA–NikE) (7), metallochaperones (e.g., UreE, HypB, CooJ) (8–10), and proteins involved in the regulation of biosynthesis (e.g., NikR, H₂ sensor) (11–13). One member of this group of proteins has been crystallographically characterized. The metallochaperone UreE was recently shown to contain two Ni-binding domains: a C-terminal polyhistidine domain involved in storing Ni, and an N-terminal domain that serves as a Ni chaperone to deliver Ni to the active site of urease (14). A recent crystal structure of the N-terminal domain with Cu²⁺ ions bound indicates that pairs of His residues are involved in binding Ni in these sites (15). XAS studies of truncated and holo proteins also reveal the importance of His ligands in constructing both the storage and chaperone sites (16–18).

An interesting example of Ni-specific uptake and the regulation thereof is provided by the Nik system in *Escherichia coli* (7,19). The Nik system comprises five proteins (NikA–NikE) that constitute a Ni-specific ATP-dependent permease, and NikR, a transcription factor that regulates the biosynthesis of the Nik permease in response to intracellular Ni concentration (11,20,21). Of the five proteins comprising the Nik permease, NikA is known to play an important role both in binding Ni and in Ni negative chemotaxis (19,22–25). Deletion of the gene encoding this protein eliminates Ni uptake and therefore the production of active hydrogenases

found in *E. coli*. The Ni-binding site in NikA has been investigated by XAS, which showed that the Ni bound to NikA is in a six-coordinate environment featuring a combination of O/N-donor ligands (26). Given the high carboxylic acid content of NikA and the similarity of the XAS spectra to those obtained from a model compound with carboxylate ligation, Ni(sal)₂(OH)₂, the data pointed to a structure with several carboxylate ligands. A recent fit of the EXAFS data using multiple scattering theory shows that the data are consistent with a site composed of two or three His imidazole ligands and three or four carboxylates (27).

The biosynthesis of the Nik permease is regulated at the transcriptional level by Fnr (fumarate nitrate regulatory protein), which activates transcription in the absence of oxygen, and by NikR, which represses the transcription of the permease in response to high (micromolar) concentrations of Ni *in vitro* (11,21). Optimal transcription is thereby achieved when the cells have a high demand for Ni—under anaerobic conditions with low concentrations of Ni.

NikR is a member of the ribbon-helix-helix family of transcription factors (20). These proteins feature homologous N-terminal domains that bind to DNA, and can have specialized C-terminal domains. The details of the DNA-binding mechanism are not completely understood. Of the known ribbon-helix-helix transcription factors, NikR is the only example that is known to respond to metal concentration. NikR is a homodimeric protein that binds as a dimer of dimers to a dyad-symmetric DNA-binding site containing a GTATGA recognition sequence repeated with separation of 16 bases. Proteins with high sequence homology to *E. coli* NikR have been identified in nine bacterial and six archaeal species. These proteins reveal the presence of six highly conserved residues (H–X₁₃–H–X₁₀–H–X–H–X₅–C–X–E) in the C-terminal domain of NikR that are associated with the presence of a high-affinity

This article is part of the monograph *Molecular Mechanisms of Metal Toxicity and Carcinogenicity*.

Address correspondence to M.J. Maroney, Dept. of Chemistry, Lederle Graduate Research Center Rm. 701, University of Massachusetts, 701 N Pleasant St, Amherst, MA 01003-9336 USA. Telephone: (413) 545-4876. Fax: (413) 545-4490. E-mail: mmaroney@chem.umass.edu

Received 1 February 2002; accepted 31 May 2002.

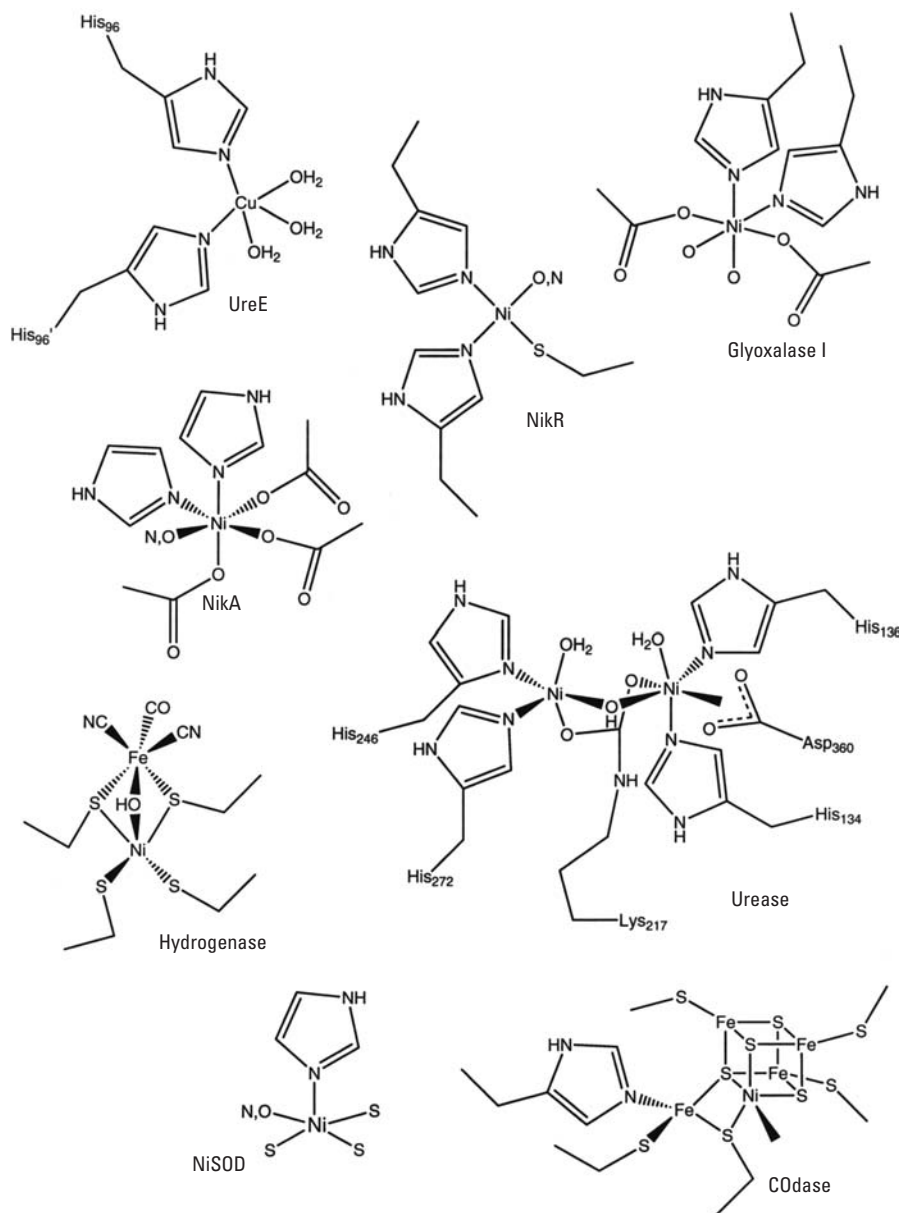


Figure 1. Examples of Ni complexes found in proteins and enzymes. The sketches are drawn using data from X-ray absorption spectroscopic and crystallographic studies (see text).

Ni-binding site ($k_d < 3$ pM). Binding of Ni to the high-affinity sites induces a conformational change in the structure of NikR that appears to be important in DNA binding. However, because the dissociation constant of this site is in the picomolar range, yet the protein represses transcription in response to micromolar levels of Ni *in vitro*, a low-affinity site is implicated. Alternatively, the distribution of Ni in the cell may be under kinetic control, in which case saturation of target Ni-binding sites would be sensed by the high-affinity Ni-binding site in NikR. Preliminary XAS analysis examining the high-affinity Ni site indicates that the protein in the absence of DNA has a planar four-coordinate Ni site featuring two histidine ligands, one S-donor

ligand (presumably cysteine), and one other O- or N-donor ligand. Thus, not all of the conserved His residues are involved in forming the high-affinity site.

A predominance of His and carboxylate ligation (Asp and Glu residues) is also found in Ni enzymes that catalyze nonredox processes. *E. coli* glyoxalase I catalyzes the isomerization of the hemimercaptal formed from the nonenzymatic reaction of glutathione and methylglyoxal into the thioester of D-lactate, which is subsequently hydrolyzed. This provides a mechanism for the detoxification of methylglyoxal by converting it to D-lactate. Crystallographic and XAS data show that the Ni site comprises two His, two Glu, and two aqua/hydroxo ligands (6,28,29).

Urease provides another well-studied example of the use of Ni in a nonredox enzyme (30). Urease is a hydrolytic enzyme that catalyzes the conversion of urea to ammonium ion and carbamate. Here, a dinuclear Ni site is bound to the protein by a combination of four His ligands and a bidentate Asp residue and bridged by a carbamate ligand formed by posttranslational carbonylation of a Lys residue (31). Each Ni is five or six coordinate, with the remaining ligands derived from water molecules in the active site (32–34).

In contrast to enzymes that catalyze nonredox reactions, cysteine ligands play a dominant role in constructing redox-active Ni sites, particularly those that use the formal Ni(III/II) redox couple (Figure 1). Hydrogenases catalyze the two-electron redox chemistry of H₂. The crystal structures of various hydrogenases reveal that the Ni-containing hydrogenases have an active-site Ni center ligated by four cysteines, two of which bridge to the Fe atom in heterodinuclear active site (35,36). In the oxidized forms of these enzymes, there is a third OH bridging group that is lost upon reductive activation of the enzyme (37). The recent crystal structures of *Carboxydotherrnus hydrogeniformans* (38) and *Rhodospirillum rubrum* (39) carbon monoxide dehydrogenases, enzymes that catalyze the two-electron redox interconversion of CO and CO₂, reveal a NiFe₄S₅ active-site cluster that incorporates a NiS₄ center formed by one cysteinato and three sulfido ligands. Superoxide dismutases catalyze the conversion of superoxide ion to oxygen and hydrogen peroxide using one-electron redox chemistry. XAS studies of Ni superoxide dismutase (NiSOD) from *Streptomyces seoulensis* shows that the Ni center giving rise to the oxidation and reduction of O₂⁻ is ligated by three S-donor ligands (40). This is true both for the resting, oxidized state, which contains a five-coordinate Ni center with one N-donor and one N- or O-donor ligand in addition to the S-donors, and for the reduced state, which has a four-coordinate Ni site with only one non-S-donor ligand. The amino acid sequence of this enzyme reveals that the protein contains only three S atoms corresponding to residues Cys₂, Cys₆, and Met₂₈. Although the involvement of the Met residue in the NiSOD active site has not been established, negatively charged S-donor ligands (thiolate and sulfide) clearly stabilize the potential of the Ni(III/II) redox couple from over +1 V for aqueous Ni ions to physiologically accessible redox potentials.

Nickel Carcinogenesis: A Structure/Function View

The details of molecular mechanism(s) that give rise to Ni carcinogenesis are not well known. Studies of Ni toxicology and carcinogenesis reveal that Ni is predominantly genotoxic and not mutagenic. These studies

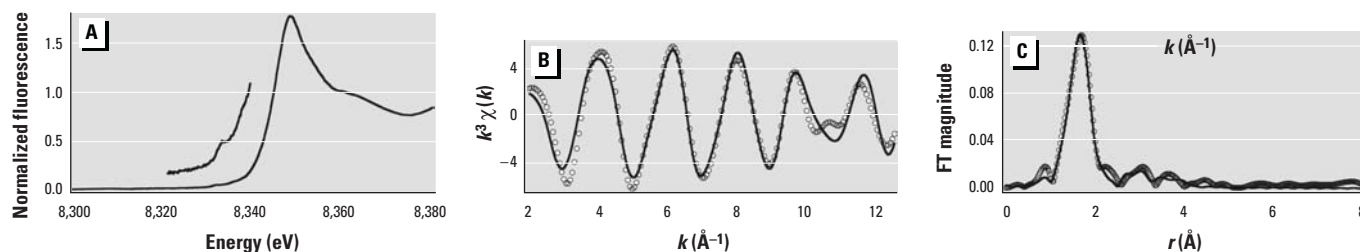


Figure 2. Ni K-edge XAS data for the Ni complex with the peptide Ac-SGRGKGGKGLGKGGAKRHRKVL-Am at pH = 9. (A) The Ni K-edge and XANES region. (B) Fourier-filtered EXAFS data (circles represent data points; solid line is the calculated fit) with Fourier transform (FT) limits = 2.0 – 12.5 Å⁻¹ and back-transformed from 1.1 to 4.2 Å. (C) Fourier-transformed EXAFS data (circles represent data points; solid line is the calculated fit) with FT limits = 2.0 – 12.5 Å⁻¹. (r = radial distance from the metal; $k = [2m_e(E - E_0)/\hbar^2]^{1/2}$, where m_e = electron mass, E = photon energy, E_0 = threshold energy of the absorption edge defined to be 8340 eV, \hbar = Planck's constant/ 2π , $\chi(k)$ = EXAFS, $k^3\chi(k)$ = EXAFS weighted by k cubed.

also show that carcinogenic Ni compounds selectively damage heterochromatin, leading to chromatin condensation and enhanced DNA methylation that silences reporter genes when they are located near heterochromatin in yeast or mammalian cells (41). There are several ways in which Ni might gain entrance into the cell. Soluble Ni compounds, which do not appear to be the principle source of carcinogenic Ni, could be transported into the cell via the Mg²⁺ transport system because of the similar charge/size ratio of the two metal ions. However, the concentration of Ni that would be required to effectively compete with Mg²⁺ transport is very high (mM) (2). Insoluble Ni compounds have been demonstrated to enter cells via endocytosis (3). The ability of Ni compounds to transform cells has been correlated to properties that increase endocytosis (e.g., particle size, charge, and solubility). Such a process is also consistent with the predominance of nasal and lung cancers caused by inhalation of insoluble Ni compounds, particularly Ni₃S₂, a potent carcinogen (2). The endocytic vesicles formed may be acidified by fusion with lysosomes, ultimately releasing large quantities of Ni ions into the cytoplasm. Further, fusion of vesicles to the nuclear membrane may deliver large quantities of Ni ions to the nucleus. Once in the nucleus, potential gene silencing, DNA base oxidation, DNA–protein cross-links, DNA gaps or breaks, and histone hydrolysis could potentially result from the interaction of Ni with DNA, histones, and/or the generation of reactive oxygen species via Ni redox chemistry or indirect effects (2).

Because Ni²⁺ ions do not bind strongly to DNA in competition with Mg²⁺, other biological complexes of Ni are implicated, and complexes formed with histone proteins are one likely target. Nuclear histones have structures consisting of globular C-terminal domains and random-coil N-terminal domains (42–45). The N-terminal tail regions are involved in internucleosome contacts and are the site of posttranslational modification via acetylation, which has been correlated with gene expression. Inspection of the amino acid sequence of

histones (46) does not reveal a large number of potential metal-binding sites because of the general lack of amino acid residues with side chains bearing Lewis bases at physiological pH. Histone H2A contains the –T₁₂₀ESHHK– sequence near the C-terminus (47). This site has a glutamic acid and two histidine residues that could engage in metal chelation. A second potentially chelating site composed of cysteine and histidine residues has been identified in the C-terminal region of histone H3: –C₁₁₀AIH– (48,49). Last, a site near the N-terminus of histone H4, –A₁₅KRHRK–, has also been proposed as a site for Ni binding largely because of the inhibitory effects of Ni on the acetylation of lysine residues near the His residue (50).

The natural biochemistry of Ni suggests that only the H3 site can possibly give rise to Ni(III/II) redox chemistry, because it is the only site with a potential cysteinate ligand that might lower the potential of this redox couple. Even this site is not likely to stabilize Ni(III/II) redox chemistry because there is only a single cysteine present. This site is also unlikely to inhibit lysine acetylation given that the location of the H3 site is in the C-terminal region. Further, the structural data regarding histones (42–45) indicate that the site is not very accessible to solvents or metals. Even though metal-centered redox chemistry can be ruled out for all but the H3 site, any of the sites could potentially activate DNA or histone proteins toward reaction with O₂, as has been suggested for the Ni site in acireductone dioxygenase (51). Each of these sites presents a unique set of ligands that could readily be distinguished by XAS provided that a homogeneous sample of a single Ni histone complex is formed. However, because of its location in the N-terminal domain, only the H4 site is likely to give rise to the changes in histone acetylation and DNA methylation that have been observed in response to Ni exposure.

The metal-binding properties of synthetic peptides that contain the –A₁₅KRHRK– H4 target Ni binding site have been studied (52). Stability constants determined for the blocked peptide Ac–AKRHRK–Am show

that >80% of Ni present in a solution at pH = 9 is bound in a single complex in solution. This complex is proposed to lead to a planar, four-coordinate, low-spin Ni tetra-aza complex formed via coordination of one His imidazole and three amide N-donor atoms.

The XAS spectrum of the Ni complex of the similar blocked peptide Ac–SGRGKGGKGLGKGGAKRHRKVL–Am, containing 22 residues beginning with the N-terminus and containing the H4 His₁₈ Ni-binding site, prepared at pH = 9, is summarized in Figure 2 (53). The Ni K-edge XANES spectrum reveals only a weak peak assigned to a 1s → 3d electronic transition [peak area = 2.6(5) × 10⁻² eV] and does not display a peak associated with a 1s → 4p_z electronic transition that is diagnostic for a planar, four-coordinate geometry. Thus, the Ni complex that is formed from this peptide under these conditions is six coordinate. EXAFS analysis shows that Ni has six O- or N-donors with an average Ni–O/N distance of 2.06(2) Å. The structure is consistent with four ligands being derived from the peptide and two originating from water. Multiple scattering analysis of EXAFS arising from atoms in the second and third coordination sphere of Ni (6) confirm that one His ligand is bound to Ni [second coordination sphere Ni–C distances averaging 3.12(5) Å, third coordination sphere Ni–C/N distances at an average of 4.26(5) Å].

Future studies are planned comparing the structure of Ni bound to histone H4 with those of this model and expectations based on other possible binding sites.

REFERENCES AND NOTES

1. Hausinger RP. Biochemistry of Nickel, Vol 12. New York:Plenum Press, 1993.
2. Oller AR, Costa M, Oberdörster G. Carcinogenicity assessment of selected nickel compounds. Toxicol Appl Pharmacol 143:152–166 (1997).
3. Costa M, Zhuang Z, Cosentino S, Klein CB, Salnikow K. Molecular mechanisms of nickel carcinogenesis. Sci Total Environ 148:191–199 (1994).
4. Colpas GJ, Maroney MJ, Bagyinka C, Kumar M, Willis WS, Suib SL, Mascharak PK, Baidya N. X-ray spectroscopic studies of nickel complexes, with application to the structure of nickel sites in hydrogenases. Inorg Chem 30:920–928 (1991).

5. Scott RA. Measurement of metal-ligand distances by EXAFS. *Methods Enzymol* 117:414–459 (1985).
6. Davidson G, Clugston SL, Honek JF, Maroney MJ. An XAS investigation of product and inhibitor complexes of Ni-containing G1x1 from *Escherichia coli*: mechanistic implications. *Biochemistry* 40:4569–4582 (2001).
7. Eitinger T, Mandrand-Berthelot MA. Nickel transport systems in microorganisms. *Arch Microbiol* 173:1–9 (2000).
8. Hausinger RP. Metallocenter assembly in nickel-containing enzymes. *J Biol Inorg Chem* 2:279–286 (1997).
9. Olson JW, Fu C, Maier RJ. The HypB protein from *Bradyrhizobium japonicum* can store nickel and is required for the nickel-dependent transcriptional regulation of hydrogenase. *Mol Microbiol* 24:119–128 (1997).
10. Watt RK, Ludden PW. The identification, purification, and characterization of CooJ. A nickel-binding protein that is co-regulated with the Ni-containing CO dehydrogenase from *Rhodospirillum rubrum*. *J Biol Chem* 273:10019–10025 (1998).
11. De Pina K, Desjardins V, Mandrand-Berthelot MA, Giordano G, Wu LF. Isolation and characterization of the nikR gene encoding a nickel-responsive regulator in *Escherichia coli*. *J Bacteriol* 181:670–674 (1999).
12. Kleihues L, Lenz O, Bernhard M, Buhrke T, Friedrich B. The H-2 sensor of *Ralstonia eutropha* is a member of the subclass of regulatory [NiFe] hydrogenases. *J Bacteriol* 182:2716–2724 (2000).
13. Bernhard M, Buhrke T, Bleijlevens B, De Lacey AL, Fernandez VM, Albracht SPJ, Friedrich B. The H-2 sensor of *Ralstonia eutropha*—biochemical characteristics, spectroscopic properties, and its interaction with a histidine protein kinase. *J Biol Chem* 276:15592–15597 (2001).
14. Brayman TG, Hausinger RP. Purification, characterization, and functional analysis of a truncated *Klebsiella aerogenes* UreE urease accessory protein lacking the histidine-rich carboxyl terminus. *J Bacteriol* 178:5410–5416 (1996).
15. Song HK, Mulrooney SB, Huber R, Hausinger RP. Crystal structure of *Klebsiella aerogenes* UreE, a nickel-binding metallochaperone for urease activation. *J Biol Chem* 276:49359–49364 (2001).
16. Colpas GJ, Brayman TG, McCracken J, Pressler MA, Babcock GT, Ming L-J, Colangelo CM, Scott RA, Hausinger RP. Spectroscopic characterization of metal binding by *Klebsiella aerogenes* UreE urease accessory protein. *J Biol Inorg Chem* 3:150–160 (1998).
17. Colpas GJ, Brayman TG, Ming L-J, Hausinger RP. Identification of metal-binding residues in the *Klebsiella aerogenes* urease nickel metallochaperone, UreE. *Biochemistry* 38:4078–4088 (1999).
18. Lee MH, Pankratz HS, Wang S, Scott RA, Finnegan MG, Johnson MK, Ippolito JA, Christianson DV, Hausinger RP. Purification and characterization of *Klebsiella aerogenes* UreE protein: a nickel-binding protein that functions in urease metallocenter assembly. *Protein Sci* 2:1042–1052 (1993).
19. Navarro C, Wu L-F, Mandrand-Berthelot M-A. The nik operon of *Escherichia coli* encodes a periplasmic binding-protein-dependent transport system for nickel. *Mol Microbiol* 9:1181–1191 (1993).
20. Chivers PT, Sauer RT. NikR is a ribbo-helix-helix DNA-binding protein. *Protein Sci* 8:2494–2500 (1999).
21. Chivers PT, Sauer RT. Regulation of high affinity nickel uptake in bacteria—Ni²⁺-dependent interaction of NikR with wild-type and mutant operator sites. *J Biol Chem* 275:19735–19741 (2000).
22. De Pina K, Navarro C, McWalter L, Boxer DH, Price NC, Kelly SM, Mandrand-Berthelot M-A, Wu L-F. Purification and characterization of the periplasmic nickel-binding protein NikA of *Escherichia coli* K12. *Eur J Biochem* 227:857–865 (1995).
23. Sawers RG, Ballantine SP, Boxer DH. Differential expression of hydrogenase isoenzymes in *Escherichia coli* K-12: evidence for a third isoenzyme. *J Bacteriol* 164:1324–1331 (1985).
24. Wu LF, Mandrand MA. Microbial hydrogenases: primary structure, classification, signatures and phylogeny. *FEMS Microbiol Rev* 104:243–269 (1993).
25. Charon M-H, Wu L-F, Piras C, de Pina K, Mandrand-Berthelot M-A, Fontecilla-Camps JC. Crystallization and preliminary X-ray diffraction study of the nickel-binding protein NikA of *Escherichia coli*. *J Mol Biol* 243:353–355 (1994).
26. Allan CB, Wu L-F, Gu Z, Choudhury SB, Al-Mjeni F, Mandrand-Berthelot M-A, Maroney MJ. An X-ray absorption spectroscopic structural investigation of the nickel site in *Escherichia coli* NikA protein. *Inorg Chem* 37:5952–5955 (1998).
27. Al-Mjeni F, Maroney MJ. Unpublished results.
28. Davidson G, Clugston SL, Honek JF, Maroney MJ. An XAS investigation of the nickel active site structure in *Escherichia coli* glyoxalase I. *Inorg Chem* 39:2962–2963 (2000).
29. He MM, Clugston SL, Honek JF, Matthews BW. Determination of the structure of *Escherichia coli* glyoxalase I suggests a structural basis for differential metal activation. *Biochemistry* 39:8719–8727 (2000).
30. Ciurli S, Benini S, Rypniewski WR, Wilson KS, Miletti S, Mangani S. Structural properties of the nickel ions in urease: novel insights into the catalytic and inhibition mechanisms. *Coord Chem Rev* 192:331–355 (1999).
31. Gabri E, Carr MB, Hausinger RP, Karplus PA. The crystal structure of urease from *Klebsiella aerogenes*. *Science* 268:998–1004 (1995).
32. Clark PA, Wilcox DE, Scott RA. X-ray absorption spectroscopic evidence for binding of the competitive inhibitor 2-mercaptoethanol to the nickel sites of Jack bean urease. A new nickel-nickel interaction in the inhibited enzyme. *Inorg Chem* 29:579–581 (1990).
33. Wang S, Lee MH, Hausinger RP, Clark PA, Wilcox DE, Scott RA. Structure of the dinuclear active site of urease. X-ray absorption spectroscopic study of native and 2-mercaptoethanol-inhibited bacterial and plant enzymes. *Inorg Chem* 33:1589–1593 (1994).
34. Yamaguchi K, Cosper NJ, Stalhandske C, Scott RA, Pearson MA, Karplus PA, Hausinger RP. Characterization of metal-substituted *Klebsiella aerogenes* urease. *J Biol Inorg Chem* 4:468–477 (1999).
35. Volbeda A, Charon MH, Piras C, Hatchikian EC, Frey M, Fontecilla-Camps JC. Crystal structure of the nickel-iron hydrogenase from *Desulfovibrio gigas*. *Nature* 373:580–587 (1995).
36. Volbeda A, Garcin E, Piras C, de Lacey AL, Fernandez VM, Hatchikian EC, Frey M, Fontecilla-Camps JC. Structure of the [NiFe] hydrogenase active site: evidence for biologically uncommon Fe ligands. *J Am Chem Soc* 118:12989–12996 (1996).
37. Davidson G, Choudhury SB, Gu ZJ, Bose K, Roseboom W, Albracht SPJ, Maroney MJ. Structural examination of the nickel site in *Chromatium vinosum* hydrogenase: redox state oscillations and structural changes accompanying reductive activation and CO binding. *Biochemistry* 39:7468–7479 (2000).
38. Dobbek H, Svetlichnyi V, Gremer L, Huber R, Meyer O. Crystal structure of a carbon monoxide dehydrogenase reveals a [Ni₄Fe₅] cluster. *Science* 293:1281–1285 (2001).
39. Drennan CL, Heo JH, Sintchak MD, Schreiber E, Ludden PW. Life on carbon monoxide: X-ray structure of *Rhodospirillum rubrum* Ni-Fe-S carbon monoxide dehydrogenase. *Proc Natl Acad Sci USA* 98:11973–11978 (2001).
40. Choudhury SB, Lee J-W, Davidson G, Yim Y-I, Bose K, Sharma ML, Kang S-O, Cabelli DE, Maroney MJ. Examination of the nickel site structure and reaction mechanism in *Streptomyces seoulensis* superoxide dismutase. *Biochemistry* 38:3744–3752 (1999).
41. Lee Y-W, Klein CB, Karagacin B, Salnikow K, Kitahara J, Dowjat K, Zhitkovich A, Christie NT, Costa M. Carcinogenic nickel silences gene expression by chromatin condensation and DNA methylation: a new model for epigenetic carcinogens. *Mol Cell Biol* 15:2547–2557 (1995).
42. Arents G, Burlingame RW, Wang B-C, Love WE, Moudrianakis EN. The nucleosomal core histone octamer at 3.1 Å resolution: a tripartite protein assembly and a left-handed superhelix. *Proc Natl Acad Sci USA* 88:10148–10152 (1991).
43. Arents G, Moudrianakis EN. DNA protein interactions in chromatin and the structure of the histone octamer. In: *Structural Biology: The State of the Art*, Proceedings of the Eighth Conversation (Sarma RH, Sarma MH, eds). Albany, NY:Adenine Press, 1994;93–108.
44. Arents G, Moudrianakis EN. The histone fold: a ubiquitous architectural motif utilized in DNA compactions and protein dimerization. *Proc Natl Acad Sci USA* 92:11170–11174 (1995).
45. Luger K, Mader AW, Richmond RK, Sargent DF, Richmond TJ. Crystal structure of the nucleosome core particle at 2.8 Å resolution. *Nature* 389:251–260 (1997).
46. von Holt C, Brandt WF, Greyling HJ, Lindsey GG, Retief FS, Rodrigues JDA, Schwager S, Sewell BT. Histone sequences. *Methods Enzymol* 170:503–523 (1989).
47. Bal W, Lukszo J, Bialkowski K, Kasprzak KS. Interactions of nickel(II) with histones: interactions of nickel(II) with CH₃CO-Thr-Glu-Ser-His-His-Lys-NH₂, a peptide modeling the potential metal binding site in the C-tail region of histone H2A. *Chem Res Toxicol* 11:1014–1023 (1998).
48. Bal W, Lukszo J, Jezowska-Bojczuk M, Kasprzak KS. Interactions of nickel(II) with histones. Stability and solution structure of complexes with CH₃CO-Cys-Ala-Ile-His-NH₂, a putative metal binding sequence of histone H3. *Chem Res Toxicol* 8:683–692 (1995).
49. Bal W, Lukszo J, Kasprzak KS. Interactions of nickel(II) with histones: enhancement of 2'-deoxyguanosine oxidation by Ni(II) complexes with CH₃CO-Cys-Ala-Ile-His-NH₂, a putative metal binding sequence of histone H3. *Chem Res Toxicol* 9:535–540 (1996).
50. Broday L, Peng W, Kuo M-H, Salnikow K, Zoroddu M, Costa M. Nickel compounds are novel inhibitors of histone H4 acetylation. *Cancer Res* 60:238–241 (2000).
51. Dai Y, Pochapsky TC, Abeles RH. Mechanistic studies of two dioxygenases in the methionine salvage pathway of *Klebsiella pneumoniae*. *Biochemistry* 40:6379–6387 (2001).
52. Zoroddu MA, Kowalik-Jankowska T, Kozlowski H, Molinari H, Salnikow K, Broday L, Costa M. Interaction of Ni(II) and Cu(II) with a metal binding sequence of histone H4: AKRHRK, a model of the H4 tail. *Biochim Biophys Acta* 1475:163–168 (2000).
53. The 22-residue peptide Ac-SGRGKGGKGLGK-GAKRHRKVL-Am was synthesized on a solid support with a 9050 Plus Synthesizer by BBM Inc. (Woburn, MA, USA) using a conventional 9-fluorenylmethoxycarbonyl (Fmoc) chemistry methodology starting from the C-terminal to the N-terminal. N-Fmoc-protected amino acids and all other peptide synthesis reagents were obtained from PE Biosystems (Applied Biosystems, Foster City, CA, USA). The peptide was purified using semipreparative high-performance liquid chromatography (HPLC) on a C₁₈ column (Varian, Inc., Palo Alto, CA, USA) eluting with 0.1% CF₃COOH-H₂O (solvent A) and 0.1% CF₃COOH-CH₃CN (solvent B) (Sigma-Aldrich S.r.l., Milano, Italy), linear gradient 0–100% B over 50 min at a 3 mL/min flow rate, with detection at 220 nm absorption used as a means of detection (Varian Vacuum Technologies, Torino, Italy). The purity of the peptide was checked by reverse-phase HPLC using a C₁₈ 5-µm 100A microsorb-MV analytical column (Alltech Associates, Inc., Deerfield, IL, USA) (4.6 mm × 25 cm; flow rate, 1 mL/min), gradient 0–50% in 25 min (solvent A, 0.1% CF₃COOH-H₂O), 50–100% in 35 min (solvent B, 0.1% CH₃CN-H₂O). The molecular weight of the peptide was confirmed by mass spectral analysis (MALDI-TOF-VOYAGER (PE Biosystems/Perseptive, Framingham, MA, USA). The Ni-peptide complex for XAS analysis was prepared by dissolving the peptide in deionized water containing 20% glycerol and adding solution containing NiCl₂ so that a 1:1 ratio of NiCl₂/peptide was achieved. The pH of this solution was adjusted to pH 9.4 by adding a dilute solution of NaOH. The concentration of the Ni-peptide complex in the sample studied was approximately 4.0 mM. The electronic absorption spectrum obtained on this sample was similar to published values for the analogous heptapeptide (52). Approximately 60 µL of the Ni-peptide solution was transferred to a polycarbonate sample holder, and frozen in liquid nitrogen. XAS data were collected at beam line X9B at the National Synchrotron Light Source, Brookhaven National Laboratories (Brookhaven, New York, USA). The polycarbonate sample holder was inserted into a slotted aluminum holder, held at 50 K. A focused X-ray beam was used, with the vertical primary slit closed down (0.2 mm) to maximize resolution in the XANES region, and opened up (1.0 mm) for intensity in the EXAFS region. The monochromator was internally calibrated to the first inflection point of Ni foil (8331.6 eV). X-ray fluorescence data were collected using a 13-element detector (Canberra, Meriden, CT, USA), and sample integrity was determined by monitored the Ni K-edge energy on sequential scans. No change in redox state or ligand environment was observed. XAS data were analyzed in analogy with previously published procedures (6) with the addition that the histidine multiple scattering pathways arising from the coordinating imidazole were correlated to the respective single scattering distances. A Fourier transform range of 2.0–12.5 Å⁻¹ and back-transform limits of 1.1–4.2 Å were used to Fourier-filter the data arising from the first coordination sphere and histidine atoms.